

ZONAL AND MERIDIONAL CIRCULATIONS IN THE EQUATORIAL ZONE AS DEDUCED FROM THE DIVERGENCE FIELD OF THE SURFACE WIND

Wang Shaowu (王绍武)

Department of Geophysics, Peking University

Todd P. Mitchell and John M. Wallace

Department of Atmospheric Sciences, University of

Washington, U.S.A.

Received June 13, 1986

ABSTRACT

The zonal and meridional circulations and their variability are examined on the basis of the surface wind data for 1950-1979. The climatological mean zonal wind and its divergence are examined in reference to the Walker Circulation. The role played by the meridional circulation in contributing to convergence of the surface wind field within the equatorial zone is emphasized. Regression coefficients are used to infer seasonal mean anomalies of divergence of the surface wind in years when the sea level pressure is 1 hPa above normal at Darwin, a condition representative of El Niño events. It is shown that anomalies in the divergence associated with the meridional wind component are primarily responsible for the heavy precipitation in the Central Pacific, while the anomalous divergence associated with the zonal wind component may cause the drought in the Western Pacific near Indonesia. A similar pattern of divergence anomalies is evident during three consecutive seasons beginning in northern summer and ending in northern winter. The reinforcement of the Hadley Circulation during El Niño episodes is noted. It is shown that the circulations over the Atlantic Ocean and Pacific Ocean are relatively uncorrelated. The interrelation between the dipole anticyclones and the meridional circulation over the central Pacific is discussed.

1. INTRODUCTION

The concept of the Walker Circulation proposed by Bjerknes (1969) is widely recognized in the meteorological community. Bjerknes' original conceptual model has been extended by Flohn and Fleer (1975) to describe the zonal circulations in the whole equatorial belt. It is believed that the Walker Circulation is weakened when El Niño events occur, and intensified during the so-called anti-El Niño periods, which are characterized by below normal SST in the equatorial eastern Pacific.

Reiter (1978) has shown that the meridional circulations over the Pacific sector are also modulated by the El Niño phenomenon. During El Niño years the meridional component of the tradewinds tends to be stronger than normal in both hemispheres over the Pacific sector, and the convergence in the equatorial zone is enhanced. Reiter showed that there is a strong positive correlation between this convergence and the rainfall in the Line Islands on the interannual timescale.

The surface wind analyses by Wright, Mitchell and Wallace (1985) arranged in seasons

for the period 1950–1979 provide a basis for a more detailed analysis of the divergence field in the equatorial zone, from which it is possible to infer the vertical motion field in the lower troposphere.

The zonal circulation identified with the Walker Circulation over the Pacific can be inferred from the zonal wind component U and its divergence. The divergence associated with the meridional wind component V , averaged around the whole latitude circles provides information concerning the Hadley Circulation. These zonal and meridional circulations are examined on the basis of the surface wind data set, with emphasis on their variability in relation to the El Niño/Southern Oscillation (ENSO) phenomenon.

II. DATA

In the report of Wright, Mitchell and Wallace (1985) all the seasonal wind component data are presented in the form of grid boxes 4° in latitude by 10° in longitude, centered at $0^\circ, 4^\circ, 8^\circ, \dots$ latitudes, and $5^\circ, 15^\circ, 25^\circ, \dots$ longitudes, in both the Northern and Southern Hemispheres. For example, the wind at $8^\circ\text{S}, 5^\circ\text{E}$ represents an average for the box $6^\circ\text{--}10^\circ\text{S}, 0^\circ\text{--}10^\circ\text{E}$. To find the average divergence for the $10^\circ\text{S}\text{--}10^\circ\text{N}$ latitude belt, the five points at $8^\circ\text{S}, 4^\circ\text{S}, 0^\circ, 4^\circ\text{N}$ and 8°N along each meridian are used. In order to make the spatial scales comparable in the zonal and meridional directions, averages for $20^\circ \times 20^\circ$ latitude-longitude boxes are calculated and assigned to the center of their respective boxes. Altogether thirty-six boxes are used with 10° longitude overlap between the boxes. The gaps in the climatological wind data set over the central Pacific and over the continents are filled using the wind estimates from Newell et al. (1972). The climatological mean divergence associated with gradients of U_n and V_n are calculated separately, and denoted as D_{U_n} and D_{V_n} , where U_n and V_n are the climatological mean zonal and meridional wind components, respectively. For studying the relationship between the divergence of the surface wind field and ENSO episodes, we used regression coefficients given in Wright, Mitchell and Wallace (1985) which show the anomalies in the wind components that should be observed when the annual mean (April through March of the following year) sea-level pressure is 1 hPa above normal at Darwin. For the purposes of this paper these conditions can be regarded as representing a typical El Niño year. The regression coefficients are presented for six seasons, namely DJF₁, MAM₁, JJA, SON, DJF₂ and MAM₂, where 1 and 2 indicate the first and the second years relative to the Darwin year as defined above; subscripts are unnecessary for JJA and SON. The grid-point format of the regression coefficients is identical to that of the climatological mean wind field described above. However, the gaps in the data have been filled in by interpolation. The divergence associated with the U and V components are denoted by D_U and D_V , respectively.

III. THE CLIMATOLOGICAL MEAN DIVERGENCE FIELD OF THE SURFACE WIND IN THE EQUATORIAL ZONE AND THE WALKER CIRCULATION

The zonal circulation in a vertical cross section along the equator, which defines the Walker Circulation, depends only upon the gradient of the U component along the equator. Therefore, as a basis for assessing the zonal circulation, we examined D_{U_n} for four successive seasons (Fig. 1A). Isopleths are drawn at $1 \times 10^{-6}\text{s}^{-1}$ intervals. Areas with the divergence (convergence) of 1×10^{-6} or more (-1×10^{-6} or less) are crosshatched (hatched). Fig. 1A shows that D_{U_n} varies little with season. Subsidence (divergence) is observed over the western Indian Ocean, the eastern Pacific and the central Atlantic. Ascent (convergence) is concentrated over

South America, the eastern Indian Ocean, the western Pacific, and Africa. In order to show more clearly the cellular structures in the zonal circulation, the zonally averaged wind component U for the latitude circle is removed, since it doesn't contribute to the divergence. The vertical motion field deduced from the divergence D_{U_m} , shown in Fig. 1A, and the zonal wind fields shown in Fig. 2A and 2C are the basis for the schematic picture of the zonal circulation shown in Fig. 2B. It is of interest to compare this schematic picture with that of Flohn and Fleer (1975). The latter is reproduced in Fig. 3A and the one based on our calculations of the divergence of the surface wind is given in Fig. 3B. Despite the general similarity between the two schematic circulations, there are some discrepancies:

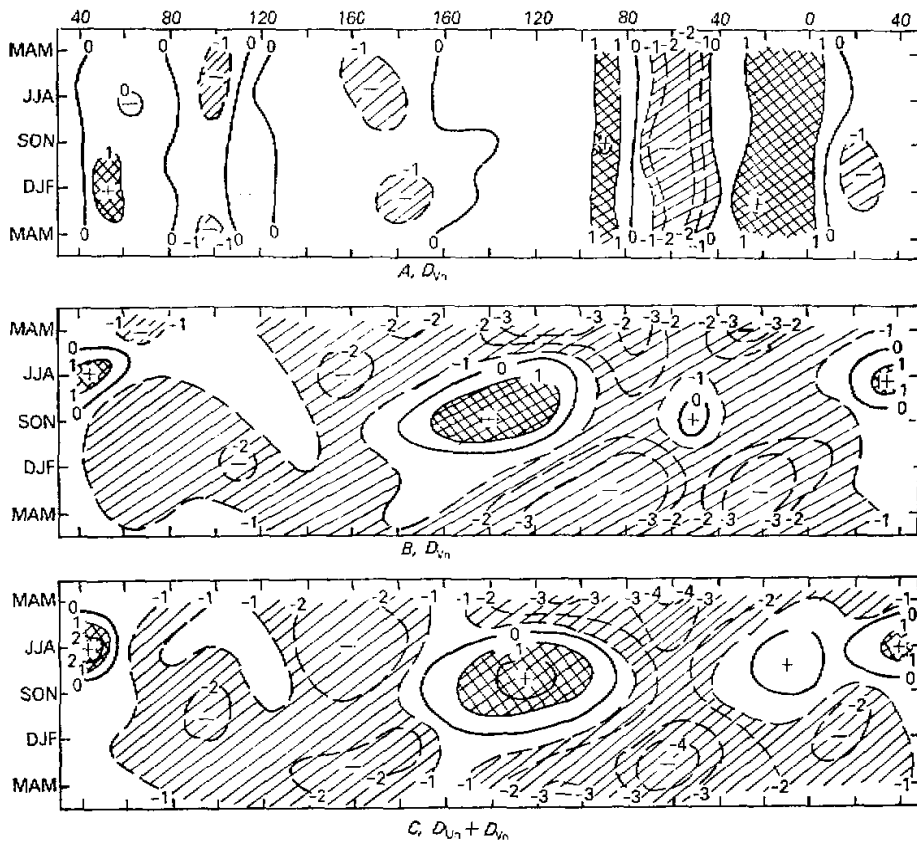


Fig. 1. Climatological mean divergence of the surface wind field in the equatorial zone 10°S-10°N in units of (10^{-6} s^{-1})

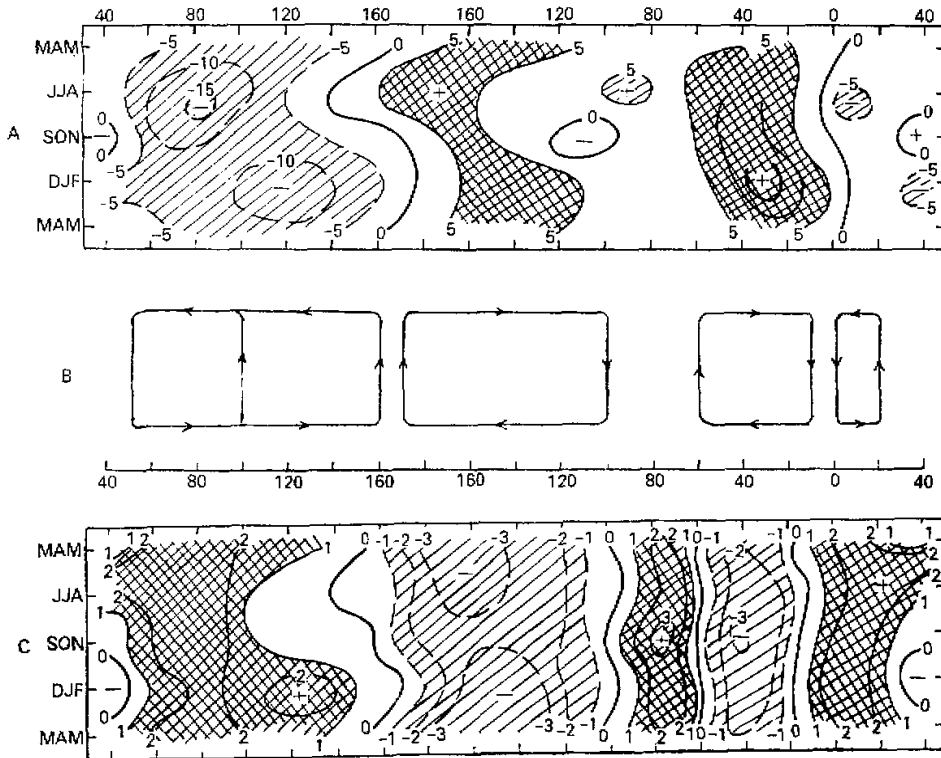


Fig. 2. Climatological mean zonal wind (A) at the 200 hPa level and (C) at the earth's surface in units of $m\ s^{-1}$. (B) Schematic picture of the circulation in the zonal plane.

(1) The cell over the Atlantic Ocean, especially its eastern part is located farther west in Fig. 3B than in Fig. 3A. The maximum divergence over the Atlantic is found to the west of the Greenwich Meridian rather than to the east of it.

(2) The cell over the Indian Ocean stretches all the way to the central Pacific along with the surface westerlies in Fig. 3B. The zero line of U at earth's surface (Fig. 2C) is near $160^{\circ}E$. Ascent (convergence) predominates for a quarter or more of the latitude circle, from $80^{\circ}E$ to $160^{\circ}W$, but the main branches of ascent are observed over Indonesia and just to the west of the Dateline.

(3) The U component at the 200 hPa level (Fig. 2A) shows westerly winds over South America and easterly winds over Africa, as indicated by the dashed arrows in Fig. 3A. Neither Fig. 2A nor Fig. 3A provides much support for a closed cell with easterly winds over South America and westerly winds over the Africa as suggested in some other schematic models. Considering the relative independence between wind variations over the Atlantic and Pacific (as will be discussed later), we prefer to draw the zonal circulations as two separate systems, each consisting of two cells. Hence, the dashed arrows shown in Fig. 3A are omitted in Fig. 3B.

(4) The shower symbols depicted in the Fig. 3A are omitted in Fig. 3B, because they give

the impression that the ascent in the equatorial zone is entirely determined by the zonal circulation, but that is not true. Fig. 1B indicates that the divergence associated with the V_n component, D_{V_n} is larger than D_{U_n} at most longitudes, so that the total divergence depends more upon D_{V_n} . The root mean square variances of the divergence associated with spatial variations of U_n and V_n are given in Table 1.

In view of the fact that the RMSSV of D_{V_n} is larger than of D_{U_n} by a factor of 2 or more, the heavy precipitation over the so-called maritime continent must be attributed to D_{V_n} rather than D_{U_n} , though the contribution of the latter can not be neglected.

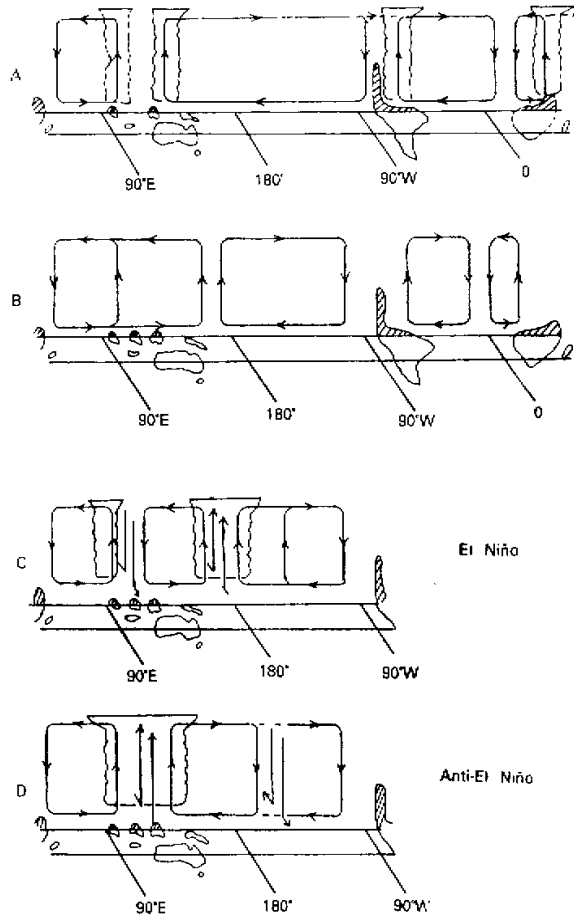


Fig. 3. Schematic zonal circulation (A) as proposed by Flohn and Fler and (B) as suggested in present paper. Modified circulations for (C) El Niño and (D) anti-El Niño episodes.

Table 1. The Root Mean Square Spatial Variance (RMSSV) of D_{U_n} and D_{V_n} , in units of $1 \times 10^{-6} s^{-1}$

RMSSV	MAM	JJA	SON	DJF
D_{U_n}	0.81	0.89	1.01	0.98
D_{V_n}	2.78	1.72	1.69	2.79

It can be concluded from the afore-mentioned analysis that the schematic picture of the zonal circulation proposed by Flohn and Fleer (1975) is generally supported by our calculations of the divergence of the surface wind field. We have made some minor modifications in the locations of the vertical branches and in the longitudinal extent of the zonal cells. However, the more important thing is to note the prominent role played by the V_n component. These meridional circulations tend to be ignored in many works which emphasize the role of the Walker Circulation in El Nino.

IV. RESPONSE OF THE EQUATORIAL DIVERGENCE FIELD TO ENSO

In studying anomalies in the divergence field associated with ENSO events, we have used regression coefficients as described in Section II. The original calculation covered only the oceans; in order to provide a more complete picture, we interpolated the streamlines of the anomalous wind field over South America and Africa. The divergences D_U, D_V , and $(D_U + D_V)$ typical of El Nino events are shown in Fig. 4. The hatched areas indicate where the divergences have been interpolated over the continents. It is clear that the features over the continents are weaker than those over the oceans, so including the interpolated values should not influence the general features very much.

Figure. 4A shows that D_U exhibits large anomalies over the Pacific and the eastern Indian Ocean from $100^\circ E$ eastward to $110^\circ W$, with convergence (indicative of ascent) towards the east and divergence (subsidence) towards the west. This situation is in general agreement with the results of previous studies of El Nino such as that of Rasmusson and Carpenter (1982). But a more detailed inspection indicates that the ascending branch is located too far to the east to be interpreted as the anomalously heavy rainfall in the central Pacific, though the subsidence in Fig. 4A coincides roughly with the area in which a deficit in precipitation is observed during El Nino events. However, the anomalous convergence associated with D_V is significant between $140^\circ E$ and 180° . In agreement with results of Reiter (1978), the maximum centered near the dateline appears to be responsible for the enhanced precipitation over the central Pacific. The greater relative importance of D_V can also be seen by comparing the root mean square spatial variances of D_V and D_U (Table 2).

Table 2. The Root Mean Square Spatial Variances of D_V and D_U , in units of $1 \times 10^{-4} s^{-1}$

RMSSV	DJF ₁	MAM ₁	JJA	SON	DJF ₂	MAM ₂
D_U	0.10	0.16	0.18	0.27	0.17	0.16
D_V	0.24	0.14	0.52	0.54	0.51	0.20

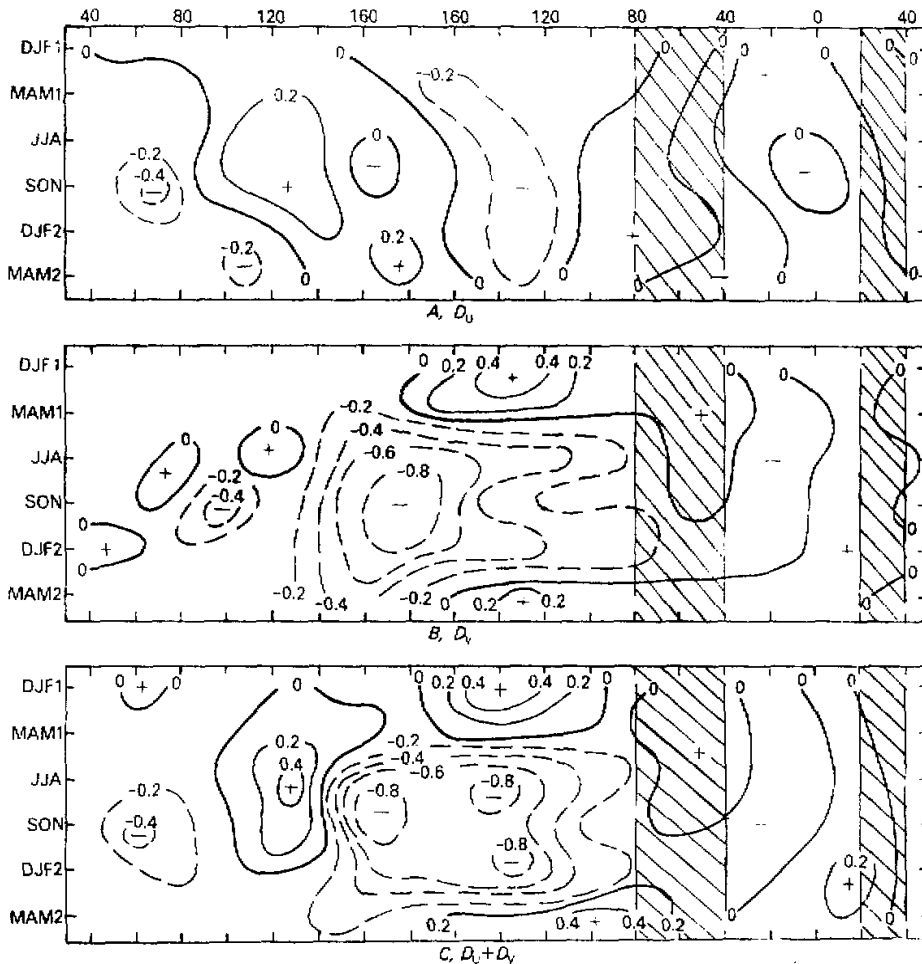


Fig. 4. Time-longitude sections of anomalies of the divergence of the surface wind field in the equatorial zone (10°S – 10°N) in years when sea level pressure (averaged from April through March) is 1 hPa above normal at Darwin, as inferred from regression coefficients (in units of 10^{-4} s^{-1}): (A) for the zonal wind component, (B) for the meridional wind component, and (C) for the total wind field.

Figure 4 and Table 2 show the strong dominance of D_v during the three seasons JJA, SON and DJF₂. In the two prior seasons, DJF₁ and MAM₂, and the later season MAM₁, D_v is smaller and opposite in sign to that observed during the three central seasons. Therefore, in subsequent parts of this paper we will tend to focus our attention on the central seasons,

Comparing Fig. 1A and Fig. 4A, it is evident that the anomalies in the divergence field tend to be of opposite sign to the climatological mean features over the Pacific. Hence, our results confirm the generally accepted notion that the Walker Circulation weakens during El Niño events. However, it is of interest to ask whether these anomalies are of sufficient amplitude to completely destroy the climatological mean Walker Circulation or even, as some authors have suggested, to give rise to an anti-Walker Circulation, with an ascending branch in the east and subsidence in the west. In order to answer this question the anomalies in Fig. 4A are averaged for the three seasons indicated above, and added to the climatological mean divergences (Fig. 1A), to obtain an estimate of the zonal circulation during El Niño episodes. Then the same anomalies are subtracted from the climatological mean field, in order to represent a typical anti-El Niño situation. The two reconstructed wind fields will be referred to as E and anti-E, respectively. Figure 5A and 5D depict the three season composite divergence field along the equator over the Pacific and Indian Oceans. The anomalies in the U component show an extension of the surface westerlies into the central Pacific (figure omitted). On the basis of these results, schematic pictures for E and anti-E episodes are presented in Fig. 5B and 5C. From Fig. 5 one can conclude that ENSO episodes do not fully destroy the climatological mean Walker Circulation because subsidence still occurs in the eastern Pacific and the ascent in the western Pacific, and subsidence again in the western Indian Ocean. The zonal circulation in both E and anti-E episodes consist of two cells—an eastern one over the Pacific and a western one over the Indian Ocean. But during E years the western cell expands eastward, accompanied by a retreat of the eastern cell. The reverse is true for anti-E conditions.

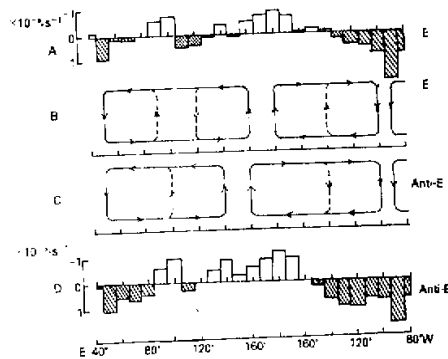


Fig. 5. Divergence averaged for JJA, SON and DJF, in contrasting years: El Niño (E) and Anti-El Niño (Anti-E). Areas of positive divergence (downward motion) are shaded. (A) $(D_{U_n} + D_U)$ during E years; (B) schematic zonal circulation during E years; (C) schematic zonal circulation during Anti-E years; and (D) $(D_{U_n} - D_U)$ during Anti-E years.

However, as indicated above, D_V is greater than D_U ; so the total anomalies of $(D_U + D_V)$, averaged for the three seasons, depend mainly upon the D_V . It is evident that the grea-

test intensification of the convergence in going from anti-E to E conditions occurs in the central and eastern Pacific. The only two areas in which the convergence is reduced are located at 110° – 140° E (near Indonesia) and at 0° – 20° E (the eastern Atlantic and West Africa). But the anomalies are small over the Atlantic and Africa. To illustrate the divergence and the inferred vertical motions associated not only with the zonal, but also with the meridional circulations, modified schemes for E and anti-E conditions are shown in Fig. 3C and 3D, where they can be compared with the climatological mean Walker Circulation.

It can be concluded that the weakening of the Walker Circulation during El Nino episodes is supported by our results, but variations of the extent of the zonal cells between E and anti-E conditions appear to be relatively more important. The cell over the Indian Ocean and the ascending branch move eastward during El Nino years, and retreat westward during anti-El Nino years. The response of the divergence associated with the V component is stronger, on average, than that associated with the U component. The heavy precipitation observed in the central Pacific during El Nino years is due, in large part, to the anomalies in D_V rather than in D_U . Our results illustrate the importance of D_V in modifying the divergence field in connection with the ENSO phenomenon. The largest response is found in the three seasons, JJA, SON and DJF₁. We believe that this seasonal dependence is linked to the seasonal variation in the zonal gradient of SST.

V. DISCUSSION

In this section the following issues are discussed: (1) the response of the Hadley Circulation to ENSO episodes, (2) the relationship between the circulation over the Pacific and Atlantic, and (3) the dipole anticyclones in the central Pacific in relation to the meridional circulation.

Figure 4 shows a tendency toward convergence at almost every longitude in the equatorial zone during El Nino years. Hence, it appears that Bjerknes (1969) was correct when he speculated that the Hadley cell is intensified during El Nino events. Apparently it is intensified, not only in the winter hemisphere as suggested by Bjerknes, but also in both hemispheres for three consecutive seasons.

The important role of meridional circulation has tended to be underemphasized in the literature because of the attractive simplicity of the two-dimensional circulation scheme embodied in the Walker Circulation. Though we don't wish to minimize the importance of the Walker Circulation as a model for interpreting the teleconnections in the equatorial zone and the mechanisms responsible for ENSO, we must point out the limited applicability of this concept. In any case, the role played by the meridional circulations can hardly be ignored.

The mean divergence anomalies for the whole latitude zone are presented in Table 3. It

Table 3. Divergence Anomalies Associated with the V Component, averaged for whole equatorial belt in units of $1 \times 10^{-4} \text{ s}^{-1}$

	DJF ₁	MAM ₁	JJA	SON	DJF ₂	MAM ₂
D_V	-0.05	-0.00	-0.21	-0.23	-0.23	-0.01
D_V/D_{Vn}	2.8%	0.0%	31.3%	38.3%	12.8%	0.6%

can be seen that the zonally averaged convergence in the equatorial belt associated with the Hadley Circulation is enhanced by as much as 30% relative to its climatological mean value during the middle seasons of El Niño episodes and it is correspondingly weakened during anti-El Niño episodes. Hence, in the months between June and November, the intensity of the Hadley cell varies by as much as 60% or more from one year to another in association with ENSO.

It is of interest to point out that the strong observed correlation between 500 hPa height averaged for the 10°–25°N latitude belt and SST in eastern equatorial Pacific must be interpreted as a reinforcement of the Hadley Circulation (Zang and Wang, 1984). During El Niño episodes the ascent increases in the equatorial zone, reinforcing the Hadley Circulation; the latter acts to intensify the subsidence in the subtropical belts, enhancing the subtropical highs in both hemispheres (Bjerknes, 1969). Therefore, strong positive correlation coefficients are observed between SST and the strength of the subtropical anticyclones.

Now we move on to the next issue: the relation between the zonal circulation over the Atlantic Ocean and ENSO. First of all, we note the close connection between the zonal circulation cell over the Indian Ocean and the one over the Pacific. Figure 4A shows the divergence anomaly between 100° and 140°E, and the convergence anomaly between 40° and 80°E. It is evident that there is an anomalous zonal cell over the Indian Ocean, with subsidence to the east and ascent to the west. This situation is in good agreement with observational and modeling results (e.g., see Julian and Chervin, 1978). The anomalous cells associated with El Niño and anti-El Niño conditions are depicted clearly by Harrison (1983). There is good reason to regard the zonal cell over the Indian Ocean as a part of the system comprising the Pacific cell.

Secondly, the SST variations and the climate anomalies over the Atlantic show different spatial characteristic from those over the Pacific. Meridional contrasts rather than zonal contrasts usually predominate (Hastenrath 1983, Moura and Kagano 1983). It has been found that most of the Sêcas (droughts in Northeast Brazil) occur during the years with cold water near and to the south of the equator and warm water to the north of the equator. At the same time, Nicholson (1983) has pointed out that precipitation in equatorial Africa tends to be below the normal in years with cold water, and above normal in years of warm water. Anomalous divergence prevails throughout the Atlantic between 5° and 10°S, but convergence is observed to the north, at 5°–10°N, when droughts occur in Northeast Brazil (Moura and Kagano, 1983). All these works emphasize meridional contrasts rather than zonal contrasts. Climatic anomalies in this region can rarely be attributed to the weakening or intensifying of the zonal circulation.

Thirdly, it is difficult to say whether El Niño-like events over the Atlantic, even if they existed, would appear simultaneously with El Niño events in the Pacific. Sometimes Sêcas appear to be linked with El Niños. El Niño years (Wang, 1985) and the Sêcas years are compared in Table 4. It can be seen that only about half the Sêcas occurred during El Niño years; so this evidence neither negates or confirms the connection between them. Moreover, the Sêcas are associated with the cold water in the South Atlantic and warm water in the North Atlantic, as opposed to warm water in the east and cold in the west as in the Pacific. In any case, for lack of strong evidence of the association between the zonal circulations over the Atlantic and Pacific, it seems appropriate to regard the zonal circulation over the Atlantic and Africa as being relatively independent of ENSO.

Table 4. El Ninos and Secas in History

	El Ninos (Wang, 1985)	Drought in NE Brazil (Moura & Shukla, 1981)	Secas (Hastenrath, 1983)
1860s	(62), 64, 68		
1870s	(71), 77—78, 77, 79		
1880s	80—81, 84, 87—88	88—89	
1890s	91, 96, 99—00	91—98	
1900s	02, 04—05	00*, 02—03, 07	
1910s	11—12, 14, 18—19	15*, 19*	15, 19
1920s	(23), 25—26		27—28
1930s	30, (35), 39—40	32—33, 36	30—32, 38—39
1940s	41, (44)	41—44*	41—44
1950s	(51), (53), 57—58	51, 53, 58*	51—53, 58
1960s	63, 65, 69		66
1970s	72, 76		70, 72, 76
1980s	82—83	80	

Finally, the meridional circulation in the central Pacific is examined. It has been shown that the biggest differences between El Nino and anti-El Nino are observed in the central Pacific and that they are mainly associated with anomalies in the meridional circulation. Streamlines of the wind anomalies defined by the regression coefficients are drawn in Fig. 6. The convergence zone between the anomalous northerly winds in the north and southerly winds in the south is striking.

In a study of the spatial characteristics of precipitation anomalies in the tropical Pacific, Wang and Ma (1986) pointed out that the first eigenvector of rainfall in the northern winter has a shape of horizontal U (\sqsubset), with a region of positive anomalies in the central equatorial Pacific, and negative anomalies to the north, south and west of it. The negative anomalies surrounding the region of enhanced rainfall indicate that rainfall is suppressed not only over the so-called maritime continent, but also in the northern and southern subtropics. The outgoing longwave radiation (OLR) anomalies in January 1983 demonstrate well the \sqsubset shape of the precipitation anomalies (Fig. 7A). The anomalies in the divergence associated with the V component during DJF₂ are shown in Fig. 7B. It can be seen that there are two belts of divergence lying roughly along 20°N and 20°S, in good agreement with the belts of below normal rainfall. The pressure regression coefficients (Wright, Mitchell and Wallace, 1985) suggest that pronounced positive sea level pressure anomalies are situated over these two belts (Fig. 7C).

Horel and Wallace (1981) have shown that these same two regions are characterized by anticyclonic anomalies at the 200 hPa level during DJF₂ of ENSO episodes (Fig. 7D). We view these anticyclones as evidence of the existence of two meridional cells, more or less symmetric about the equator, with the subsidence branches in the subtropics. The prominence of this pattern suggests that the extensive ascent of air in the central Pacific is compensated, not only by divergence over the maritime continent, but also from both north and south. This meridional circulation is an important supplement to the two-dimensional Walker Circulation scheme (see Fig. 3C and 3D).

It must be noted that the results presented here are mainly based on surface wind

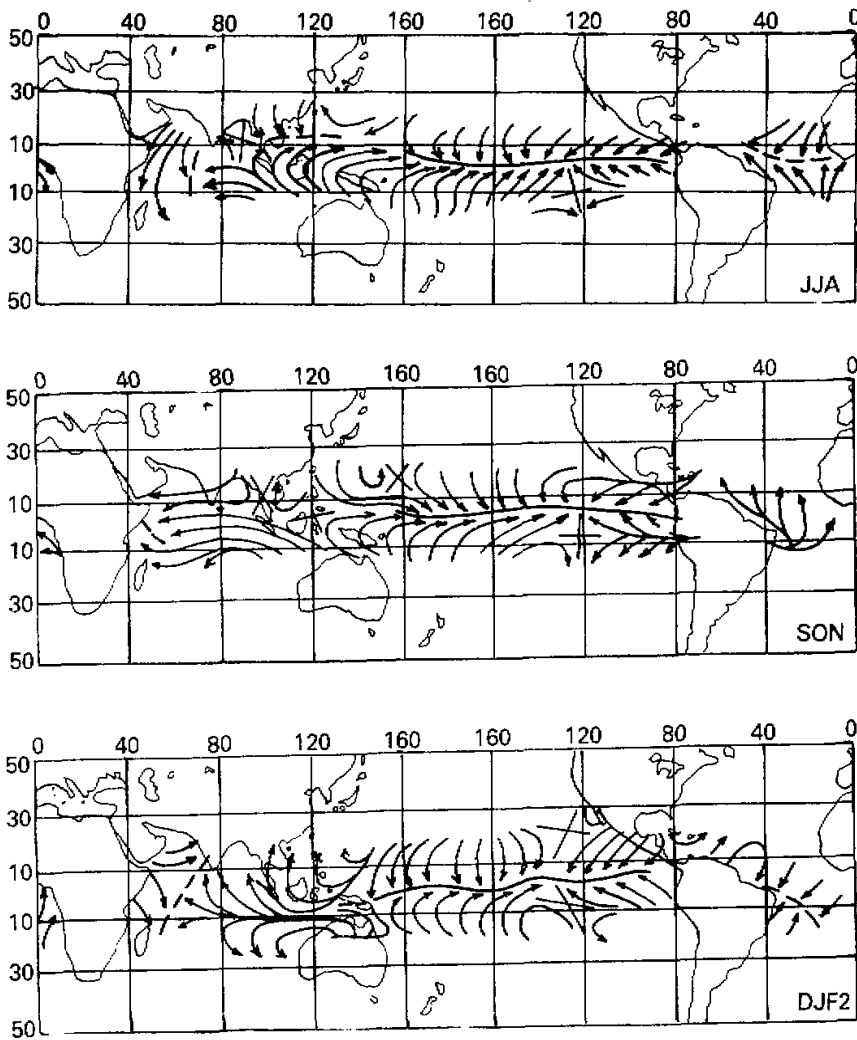


Fig. 6. Streamlines of the **anomalous** surface wind field based on the wind regression coefficients for Darwin sea-level pressure for March through February of El Niño years.



Fig. 7. (A) OLR anomalies during January 1983 ($w m^{-2}$); (B) D_V during DJF₂ in units of $10^{-6} s^{-1}$; (C) pressure regressions for DJF₂ in units of hPa per hPa of sea-level pressure anomaly at Darwin; and (D) 200 hPa streamfunction anomalies during January 1983.

data. It is well known that wind patterns vary with height, so that care must be taken in inferring the vertical velocity field in the middle troposphere on the basis of the divergence of the surface wind field alone. In particular, there is evidence that the wind field becomes relatively more zonal as one ascends above the planetary boundary layer. For example, in the 850 hPa analyses in the *Climate Diagnostics Bulletin* published monthly by the U.S. National Meteorological Center, the zonal wind component tends to dominate the circulation in the equatorial belt and the convergence of the meridional wind component toward the equator is not as pronounced as in the surface wind field. Harrison and Gutzler (1986) have shown that the zonal wind speeds tend to increase more rapidly with height than the meridional wind speeds; the ratio of the temporal variances of the U and V components in monthly mean data increases from about 1 at the earth's surface to about 3 at the 850 hPa level at an island station in the equatorial Pacific. Hence, it is possible that the circulations in the zonal plane such as the Walker Circulation play a more prominent role in the wind and vertical velocity patterns in the free atmosphere than our analysis would tend to indicate.

REFERENCES

- Bjerknes, J. (1969), Atmospheric teleconnections from the equatorial Pacific. *Mon. Wea. Rev.*, **97**: 163-172.
- Climate System Monitoring (1985), The Global Climate System. World Climate Data Programme, World Meteorological Organization, Geneva, 52pp.
- Flohn, H. and Fleer, H. (1975), Climatic teleconnections with the equatorial Pacific and the role of Ocean/Atmosphere coupling. *Atmosphere*, **13**:96-109.
- Harrison, M.S.J. (1983), The southern oscillation, zonal equatorial circulation cells and South African rainfall. *First International Conference on Southern Hemisphere Meteorology, July 31-August 6*, 302-305.
- Harrison, D.E. and Gutzler, D.S. (1986), Variability of monthly averaged surface and 850 hPa winds at tropical Pacific islands. *Mon. Wea. Rev.*, **114**, 285-294.
- Hastenrath, S. and Heller, L. (1977), Dynamics of climatic hazards in Northeast Brazil. *Quart. J. Roy. Meteorol. Soc.*, **103**:77-92.
- Hastenrath, S. (1983), Towards the monitoring and prediction of Northeast Brazil droughts. *First International Conference on Southern Hemisphere Meteorology, July 31-August 6*:116-119.
- Horel, J.D. and Wallace J.M. (1981), Planetary scale atmospheric phenomena associated with the Southern Oscillation. *Mon. Wea. Rev.*, **109**:813-829.
- Julian, P.B., and Chervin, R.M. (1978), A study of Southern Oscillation and Walker Circulation phenomenon. *Mon. Wea. Rev.* **106**: 1433-1451.
- Moura, A.D. and Kagano, M.T. (1983), Teleconnections between South America and Western Africa as revealed by monthly precipitation analyses, *First International Conference on Southern Hemisphere Meteorology, July 31-August 6* **6**: 120-122.
- Moura, A.D. and Shukla, J. (1981), On the dynamics of droughts in Northeast Brazil; Observations, theory and numerical experiments with a general circulation model. *J. Atmos. Sci.*, **38**:2653-2675.
- Newell, R.E., Kidson, J.W., Vincent, D.G. and Boer, G.J. (1972), The general circulation of the extratropical latitudes, Vol. 1, M.I.T. Press, 258pp.
- Nicholson, S.E. (1983), Rainfall fluctuations in Africa-interhemispheric teleconnections. *First International Conference on Southern Hemisphere Meteorology, July 31-August 6*: 123-126.
- Rasmusson, E.M., and Carpenter, T.H. (1982), Variations in tropical sea surface temperature and surface wind fields associated with the Southern Oscillation/El Nino, *Mon. Wea. Rev.*, **110**:354-384.
- Reiter, E.R. (1978), Long term wind variability in the tropical Pacific, its possible causes and effects. *Mon. Wea. Rev.*, **106**:324-330.
- Shukla, J. and Wallace, J.M. (1983), Numerical simulation of the atmospheric response to equatorial Pacific sea surface temperature anomalies. *J. Atmos. Sci.*, **40**:1613-1630.
- Wang Shaowu (1985), The El Nino events in 1860-1979. *Kexue Tongbao*, **30**:927-931.
- Wang Shaowu, Ma Liang and Chen Zhenhua (1986), The western and central Pacific rainfall and the El Nino events, *Acta Meteorologica Sinica*, **44**: 403-410.

-
- Wright, P.B. Mitchell, T.P. and Wallace, J.M., (1985), Relationships between surface observations over the global oceans and the southern oscillation. NOAA Data Report ERL PMEL-12, Pacific Marine Environmental Laboratory, Seattle, Washington, 61pp.
- Zang Hengfan and Wang Shaowu (1984), Equatorial eastern Pacific SST and the subtropical highs. *Acta Oceanologica Sinica*, 3: 471-476.